# Two-Stage Interpolation Algorithm for Precise Frequency Estimation of Vibration Signals

**Jean Louis NTAKPE**
*"Eftimie Murgu" University of Resita, Department of Mechanical Engineering, P-ta Traian Vuia 1-4, 320085 Resita, ROMANIA, l.ntakpe@uem.ro*

**Gilbert-Rainer GILLICH**
*"Eftimie Murgu" University of Resita, Department of Mechanical Engineering, P-ta Traian Vuia 1-4, 320085 Resita, ROMANIA, gr.gillich@uem.ro*

**Andea Amalia MINDA**
*"Eftimie Murgu" University of Resita, Department of Electrical Engineering and Informatics, P-ta Traian Vuia 1-4, 320085 Resita, ROMANIA, a.minda@uem.ro*

**Ion Cornel MITULETU**
*"Eftimie Murgu" University of Resita, Department of Electrical Engineering and Informatics, P-ta Traian Vuia 1-4, 320085 Resita, ROMANIA, mituic@yahoo.com*

**Nicoleta GILLICH**
*"Eftimie Murgu" University of Resita, Department of Electrical Engineering and Informatics, P-ta Traian Vuia 1-4, 320085 Resita, ROMANIA, n.gillich@uem.ro*

*Abstract:* - We present in this paper a simple approach to estimate the frequency components of a signal acquired from a freely vibrating structure. A non-contact excitation technique with a controlled bandwidth is involved, which is obtained by employing a loudspeaker producing for a short time a *sine* signal. This excitation ensures a strong harmonic component in the frequency range of interest and low components outside this range. In this way, the component of interest is not polluted by noise. The relevant portion of the response signal is extracted for spectral analysis. First, an interpolation by applying zero-padding in order to double the number of the spectral bins is performed. In this way, the main lobe in the spectrum contains four points. Based on three of these points a polynomial interpolation is applied and the function crossing the points is found. The maximum is presumed to be the magnitude, while its ordinate is considered the natural frequency. Simulations involving a generated pure *sine* confirm the precision achieved by this method.

*Keywords:* - frequency estimation, DFT, zero-padding, interpolation, natural frequency

## 1. INTRODUCTION

Precise frequency estimation is a demand in damage detection because structural changes lead to small frequency shifts. For this reason, numerous attempts to improve frequency readability were developed in time [1-5], but these are either complicated or not precise enough.

The main problem if natural frequencies are targeted is the rapid signal damping. The short signal resulted ensures widespread spectral bins, thus a poor frequency resolution. If the signal's harmonic component does not fit the spectral bin, the frequency and magnitude are incorrectly indicated. The magnitude is always diminished, while the frequency is indicated at the left or the right of the true one, depending where the closest spectral bin is located. The phenomenon is known as leakage.

Improving the frequency readability means finding the evaluated frequency as close as possible to the true one. The most methods concerning this issue bases on the property that the magnitude achieves the highest value if the spectral bin fits the real frequency. In consequence, interpolation may be a solution, but the problem is that just two points are always present on the main lobe in the spectrum. Therefore, a series of interpolation methods concerning two points were developed, see for instance [6-8]. On the other hand, approaches that consider three points are also present in the literature [9-11]. A critical review is made in papers [12-14].

In this paper, we propose a frequency estimation method, applicable to engineering structures, which increases the number of points in the main lobe of the spectrum and permits achieving accurate results.

## 2. CRITICAL REVIEW OF ACTUAL INTERPOLATION METHODS

The results achieved by employing standard frequency evaluation methods are in direct connection with the position of the spectral bins, as shown in Figure 1. Here, the true frequency is marked with a dashed green line, while the frequencies indicated in the spectrum are plotted with continuous grey lines. See for instance the maximizer, i.e. the peak magnitude $A_j$ associated with the spectral bin index $j$. It has the neighbor spectral bins $j-1$ and $j+1$ which indicate the magnitudes $A_{j-1}$ and $A_{j+1}$. The true frequency is close to the maximizer, but it is located at an inter-bin position. The magnitude designated here is $A$, which is the magnitude of the harmonic signal.

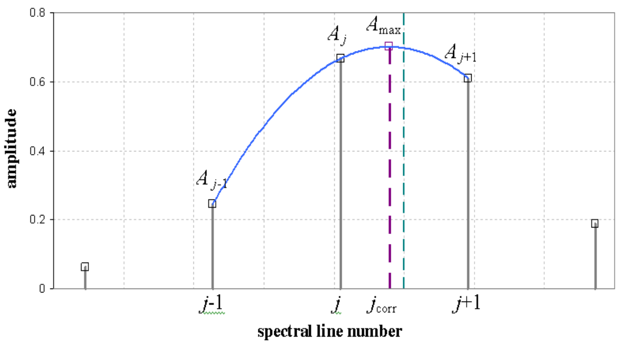


**Figure 1.** DFT output for a sine signal by standard frequency evaluation method

To find the true frequency at an inter-bin position relies on finding the maximum of the curve containing several points indicated in the DFT. To this aim, a fractional correction term $\delta$ is involved. It defines the distance between the maximizer's bin $j$ and the inter-bin position $j_{corr}$ at which the curve obtained by interpolation get the highest magnitude $A_{max}$. Evidently, the positions of $j_{real}$ and $j_{corr}$ should be as close as possible [12].

Once the term $\delta$ is found, $f_{corr}$ is calculated by adjusting the coarse estimated frequency $f_j = j\,\Delta f$ with the fraction of the frequency resolution $\Lambda f = \delta\,\Delta f$ in concordance with $\delta$. The estimation involving displacement $\delta$ is referred to as fine frequency estimation [15].

Several interpolation methods, involving the DFT maximizer $A_j$ and its largest two neighbors, are briefly presented below. The methods considering two points make use of the largest neighbor to find first the magnitude ratio and afterwards the correction term. For these methods, the bigger neighbor is always taken in consideration. Finally, the frequency is derived involving the correction term. Tables 1 and 2 indicate the mathematical relations used to find the corrected frequencies.

**Table 1.** Interpolation algorithms based on two points

| Grandke [6] | | |
|---|---|---|
| magnitude ratio | correction term | corrected frequency |
| $\alpha = \dfrac{A_{j-1}}{A_j}$ | $\delta = \dfrac{2\alpha - 1}{\alpha + 1}$ | $f_{corr} = (j + \delta)\Delta f$ |
| $\alpha = \dfrac{A_{j+1}}{A_j}$ | | $f_{corr} = (j + 1 + \delta)\Delta f$ |

| Quinn [7] | | |
|---|---|---|
| $\alpha_1 = \dfrac{A_{j-1}}{A_j}$ | $\delta_1 = \dfrac{\alpha_1}{1 - \alpha_1}$ | $f_{corr} = (j + \delta)\Delta f$ |
| $\alpha_2 = \dfrac{A_{j+1}}{A_j}$ | $\delta_2 = \dfrac{-\alpha_2}{1 - \alpha_2}$ | |
| if $\lvert\delta_1\rvert > \lvert\delta_2\rvert$ then $\delta = \delta_2$ ; else $\delta = \delta_1$ | | |

| Jain et al. [8] | | |
|---|---|---|
| $\alpha_1 = \dfrac{A_j}{A_{j-1}}$ | $\delta_1 = \dfrac{\alpha_1}{1 + \alpha_1}$ | $f_{corr} = (j - 1 + \delta_1)\Delta f$ |
| $\alpha_2 = \dfrac{A_{j+1}}{A_j}$ | $\delta_2 = \dfrac{-\alpha_2}{1 - \alpha_2}$ | $f_{corr} = (j + \delta)\Delta f$ |

**Table 2.** Interpolation algorithms based on three points

| Ding et al. [9] | |
|---|---|
| correction term | corrected frequency |
| $\delta = \dfrac{A_{j+1} - A_{j-1}}{A_{j-1} + A_j + A_{j+1}}$ | $f_{corr} = (j + \delta)\Delta f$ |

| Voglewede [10] | |
|---|---|
| $\delta = \dfrac{A_{j+1} - A_{j-1}}{2\left(2A_j - A_{j-1} - A_{j+1}\right)}$ | $f_{corr} = (j + \delta)\Delta f$ |

| Jacobsen and Kootsookos [11] | |
|---|---|
| $\delta = \dfrac{A_{j+1} - A_{j-1}}{2A_j - A_{j-1} - A_{j+1}}$ | $f_{corr} = (j + \delta)\Delta f$ |

**Table 3.** DFT outcomes for the harmonic signal: the magnifier and its two neighbors

| t [s] | Δf | $f_{j-1}$ | $A_{j-1}$ | $f_j$ | $A_j$ | $f_{j+1}$ | $A_{j+1}$ |
|---|---|---|---|---|---|---|---|
| **0.9** | 1.111111 | 3.332963 | 0.254574 | 4.443951 | 0.673429 | 5.554938 | 0.603752 |
| **0.92** | 1.086957 | 4.347354 | 0.53286 | 5.434192 | 0.732003 | 6.52103 | 0.19372 |
| **0.94** | 1.06383 | 4.254867 | 0.377557 | 5.318583 | 0.850864 | 6.3823 | 0.191731 |
| **0.96** | 1.041667 | 4.166233 | 0.227692 | 5.207791 | 0.941752 | 6.249349 | 0.161721 |
| **0.98** | 1.020408 | 4.081216 | 0.10006 | 5.10152 | 0.991773 | 6.121824 | 0.096408 |
| **1** | 1 | 3.9996 | 0.000444 | 4.9995 | 0.99995 | 5.9994 | 0.000546 |
| **1.02** | 0.980392 | 3.921184 | 0.081233 | 4.90148 | 0.975533 | 5.881776 | 0.117233 |
| **1.04** | 0.961538 | 3.845784 | 0.151012 | 4.80723 | 0.929547 | 5.768676 | 0.240323 |
| **1.06** | 0.943396 | 3.773229 | 0.208323 | 4.716536 | 0.865856 | 5.659843 | 0.362305 |
| **1.08** | 0.925926 | 3.703361 | 0.242969 | 4.629201 | 0.779911 | 5.555041 | 0.48409 |
| **1.1** | 0.909091 | 3.636033 | 0.24564 | 4.545041 | 0.666297 | 5.45405 | 0.609578 |

Figures 2 and 3 illustrate the accuracy of the interpolation methods for a sinusoid with the frequency $f = 5\,\text{Hz}$, if the signal time length varies between 0.9 and 1.1 seconds. The frequency-magnitude pairs extracted via DFT for the maximizer and the two neighbors are indicated in Table 3.

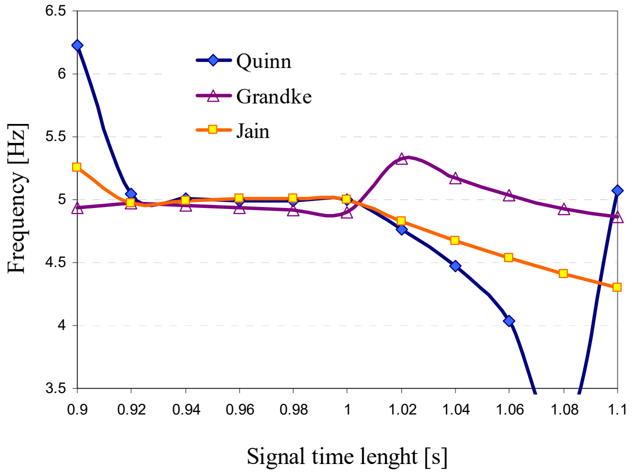


**Figure 2.** Accuracy of interpolation methods that consider two points in the DFT

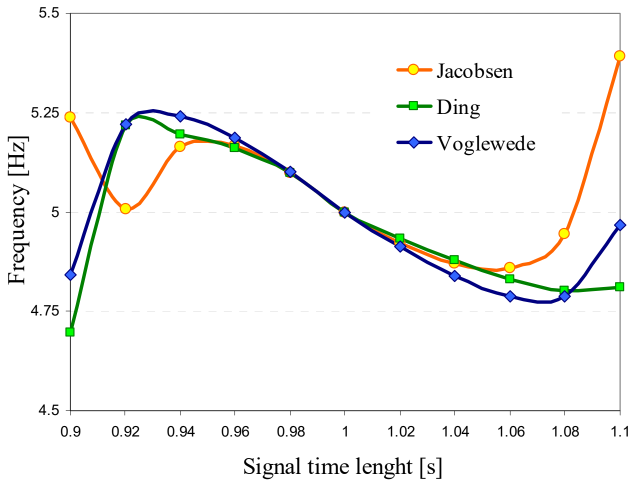


**Figure 3.** Accuracy of interpolation methods that consider three points in the DFT

From these figures can be deduces that the correct frequency is found if the signal contains entire number of cycles, i.e. $t = 1\,\text{s}$, in all other cases deviation from the correct value is observed [14]. This deviation is in range of ±10% for the methods considering two points and ±5% for the methods considering three points for interpolation. Though, for a large analysis time domain the results obtained by interpolation using two points are pretty close to the real frequency.

## 3. PROBLEM SOLUTION

The weakness of the above-presented frequency estimators is that just two points marked with blue color belong to the main lobe, as indicated by white squares in Figure 4.

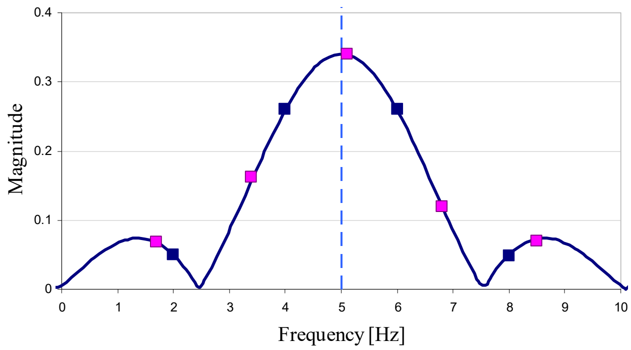


**Figure 4.** DFT representation of the original signal (blue squares) and of the resulted signal after 1:X zero-padding (magenta squares). The main lobe and the side-lobes are plotted using the absolute *sinc* function.

Processing the signal by zero-padding before interpolation, a technique not mentioned in the literature as far as the authors know, is an available option to improve frequency readability. Increasing the number of samples by zero-padding ensures more points in the main lobe, marked with magenta squares In Figure 4. Additional points on the main lobe make the interpolation more efficient.

**Table 4.** DFT outcomes for the zero-padded signal: the magnifier and its two neighbors

| t [s] | Δf [Hz] | $f_{j-1}$ [Hz] | $A_{j-1}$ | $f_j$ [Hz] | $A_j$ | $f_{j+1}$ [Hz] | $A_{j+1}$ |
|---|---|---|---|---|---|---|---|
| **1.8** | 0.555556 | 4.444444 | 0.337034 | 5 | 0.5 | 5.555556 | 0.301557 |
| **1.84** | 0.543478 | 4.347826 | 0.266746 | 4.891304 | 0.487444 | 5.434783 | 0.365745 |
| **1.88** | 0.531915 | 4.255319 | 0.189083 | 4.787234 | 0.464673 | 5.319149 | 0.425242 |
| **1.92** | 0.520833 | 4.6875 | 0.433634 | 5.208333 | 0.470754 | 5.729167 | 0.180509 |
| **1.96** | 0.510204 | 4.591837 | 0.391526 | 5.102041 | 0.495834 | 5.612245 | 0.240681 |
| **2** | 0.5 | 4.5 | 0.335063 | 5 | 0.5 | 5.5 | 0.303152 |
| **2.04** | 0.490196 | 4.411765 | 0.265221 | 4.901961 | 0.487876 | 5.392157 | 0.36693 |
| **2.08** | 0.480769 | 4.326923 | 0.188505 | 4.807692 | 0.464965 | 5.288462 | 0.425596 |
| **2.12** | 0.471698 | 4.716981 | 0.433186 | 5.188679 | 0.470468 | 5.660377 | 0.18078 |
| **2.16** | 0.462963 | 4.62963 | 0.390256 | 5.092593 | 0.495465 | 5.555556 | 0.241685 |
| **2.2** | 0.454545 | 4.545455 | 0.333467 | 5 | 0.5 | 5.454545 | 0.30447 |

More points on the main lobe occur because zero-padding does not increase the frequency resolution but brings more bins in the spectrum without increasing the frequency domain.

The layout of the DFT outcomes for the original and the zero-padded signal are illustrated in Figure 4. It is worth mentioning that by zero-padding the magnitudes indicated at the spectral bins are smaller in comparison with that indicated for the original signal, because the energy is spread over an increased number of spectral bins. To make the DFT outcomes comparable, the magnitudes of the zero-padded signal in Figure 4 are multiplied with X. The original frequencies and magnitudes for the zero-padded signal are presented in Table 4.

The function on which the main lobe is constructed is the *sinc* function [12], which can be replaced, if just the main lobe is targeted, by a quadratic polynomial. The second interpolation stage consists in finding the polynomial crossing trough three points belonging to the main lobe and deriving its maxima. The abscissa associated to the maxima is considered the corrected frequency.

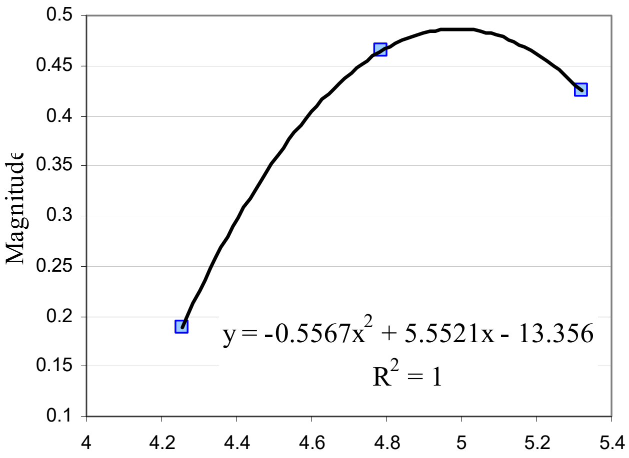


**Figure 5.** Interpolation based on three points of the main spectral lobe with indicating the regression function

**Table 5.** Corrected frequencies and achieved errors

| t [s] | Δf [Hz] | $f_{corr}$ [Hz] | Error [%] |
|---|---|---|---|
| **1.8** | 0.555556 | 4.972588 | 0.54824 |
| **1.84** | 0.543478 | 4.969979 | 0.60042 |
| **1.88** | 0.531915 | 4.986618 | 0.26764 |
| **1.92** | 0.520833 | 5.006961 | -0.13922 |
| **1.96** | 0.510204 | 4.994642 | 0.10716 |
| **2** | 0.5 | 4.97775 | 0.445 |
| **2.04** | 0.490196 | 4.974266 | 0.51468 |
| **2.08** | 0.480769 | 4.988144 | 0.23712 |
| **2.12** | 0.471698 | 5.006396 | -0.12792 |
| **2.16** | 0.462963 | 4.997074 | 0.05852 |
| **2.2** | 0.454545 | 4.981739 | 0.36522 |

Figure 5 shows the regression curve constructed on three points found in the DFT for the analysis time length of 1.88 seconds. All corrected frequencies found for the zero-padded signals are given in Table 5, where also the errors shown. From this table one can observe that errors do not exceed 1% that proves the high precision achieved if estimating the frequencies by the proposed method.

## 4. PRECISION TEST ON A MEASURED SIGNAL

It is important to ensure high precision in evaluating frequencies for real-world signals, as those acquired from vibration measurements. An eloquent example how the two-stage interpolation algorithm is employed to perform this is comprehensively presented in this section.

The way how the excitation is applied dramatically influences the measurement results. In order to achieve a low signal-to-noise ratio (SNR), in this example the excitation is provided by a system able to ensure a controlled sound pressure. The experimental bench including the non-contact excitation system is shown in Figure 6, while the computational equipment is presented in Figure 7.

**Figure 6.** Test bench with sound pressure generator

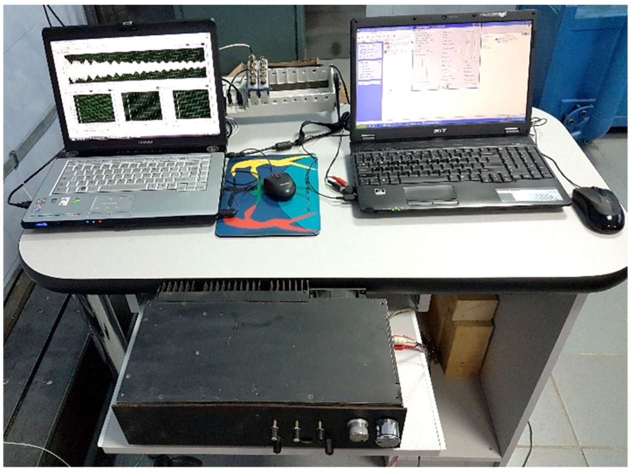

**Figure 7.** Computational equipment to generate the excitation signal and acquire the vibration response

The excitation technique consists in generating a short-time harmonic signal with the frequency quite close to the frequency of interest. To this aim, the signal generator installed on the laptop shown on the right side of Figure 7 is used. The signal is amplified by the device present at the bottom of Figure 7 and is afterwards transmitted to the loudspeaker shown in Figure 6. It is placed in front of one of the cantilever beam's anti-nodes belonging to the measured vibration mode. By this technique the energy is concentrated in a narrow frequency bandwidth. Therefore, the beam vibrates mainly in the excited mode, for all other modes the magnitudes being insignificant.

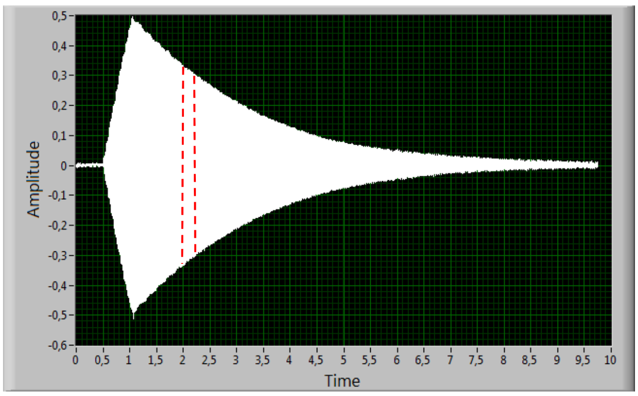


**Figure 8.** Typical vibration signal acquired during excitation and following free vibration

Typical vibration response to a short harmonic excitation (0.6 seconds) is presented in Figure 8. After the excitation has ceased, the beam is subject of a free damped vibration, thus the amplitudes decrease.

A signal portion extracted from the signal sector corresponding to the free vibration is presented in Figure 9. The signal is very little influenced by other harmonic components, thus a very low SNR is present. This makes finding the searched harmonic component easy, as shown in Figure 10. One can observe that frequencies of the first and second mode (at the left side of the relevant spectral bin) and superior modes (at the right side) are not visible since their magnitudes are extremely small.

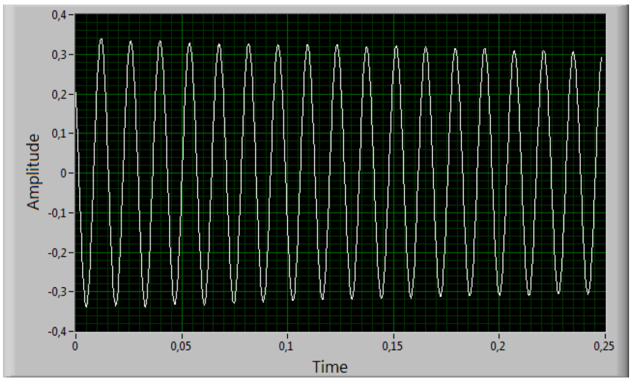


**Figure 9.** Extracted signal portion from the free vibration

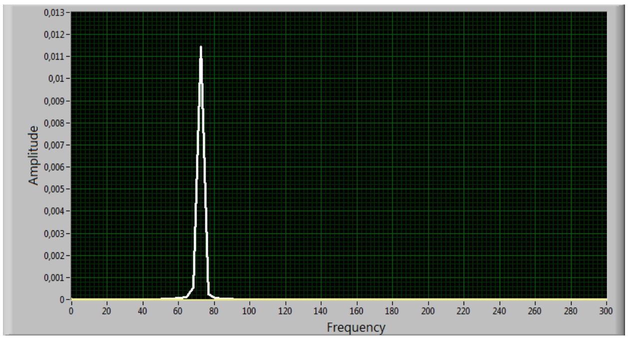


**Figure 10.** The main lobe in the spectrum; notice that other harmonic components are not observable

If the extracted signal portion of length 0.25s is zero-padded with additional 0.25s, four points are indicated in the spectrum. The maximizer and its two neighbors are indicated in table 6. Here, also the corrected frequency achieved after interpolation is indicated.

**Table 6.** DFT outcomes and the corrected frequencies

<table>
<tr><td>$f_{j-1}$ [Hz]</td><td>69.08041</td><td rowspan="6">$f_{corr}$ [Hz]</td><td rowspan="6">71.6136</td></tr>
<tr><td>$A_{j-1}$</td><td>0.068088</td></tr>
<tr><td>$f_j$ [Hz]</td><td>71.11219</td></tr>
<tr><td>$A_j$</td><td>0.154338</td></tr>
<tr><td>$f_{j+1}$ [Hz]</td><td>73.14397</td></tr>
<tr><td>$A_{j+1}$</td><td>0.131748</td></tr>
</table>

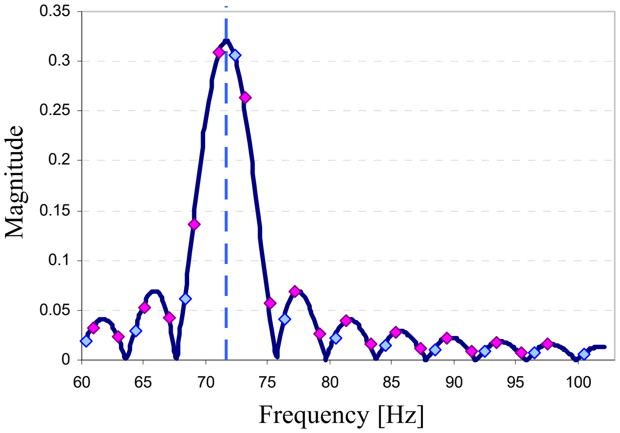


**Figure 11.** Diagram showing the frequency-magnitude pairs belonging to the main lobe

The points representing the frequency-magnitude pairs for the extracted and zero-padded signals are presented in Figure 11. The DFT points are superposed on the *sinc* function. To facilitate comparison, the magnitudes of the zero-padded signal are multiplied by two. From Figure 11 clearly results that for the original signal two points (blue rhombuses) belong to the main lobe, while doubling the analysis time by zero-padding four points (pink rhombuses) have this property. Taking the three relevant points, interpolation is successfully performed.

## 5. CONCLUSIONS

The proposed algorithm, consisting in zero-padding a signal and performing a polynomial interpolation base on three relevant DFT points belonging to the main lobe is simple to be applied and the process can be automated. Tests performed on generated as well as on real-world signals have proved its robustness and reliability. It is important to mention that the results are not influenced by the sampling rate or acquisition time, dissimilar with those achieved by applying the algorithms existing in the literature. For the generated signal the errors were less than 1%.

## ACKNOWLEDGMENTS

The work has been funded by the Sectoral Operational Programme Human Resources Development 2007-2013 of the Ministry of European Funds through the Financial Agreement POSDRU/159/1.5/S/132395.

## REFERENCES

[1] Rife D., Boorstyn R., Single-tone parameter estimation from discrete-time observations, *IEEE Transactions on Information Theory*, Vol. 20, No. 5, 1974, pp. 591–598.

[2] Onchis-Moaca D., Gillich G.R., Frunza R., *Gradually improving the readability of the time-frequency spectra for natural frequency identification in cantilever beams*, 2012 Proceedings of the 20th European Signal Processing Conference (EUSIPCO), 2012, pp. 809-813.

[3] Aboutanios E., Mulgrew B., Iterative frequency estimation by interpolation on Fourier coefficients, *IEEE Transactions on Signal Processing*, Vol. 53, No. 4, 2005, pp. 1237–1242.

[4] Tretter S., Estimating the frequency of a noisy sinusoid by linear regression, *IEEE Transactions on Information Theory*, Vol. 31, No. 6, 2002, pp. 832–835.

[5] Gillich N., Mituletu I.C., Gillich G.R., Chioncel C.P., Hatiegan C., Frequency and magnitude estimation in voltage unbalanced power systems, *10th International Symposium on Advanced Topics in Electrical Engineering (ATEE)*, 2017, pp. 1-4.

[6] Grandke T., Interpolation Algorithms for Discrete Fourier Transforms of Weighted Signals, *IEEE Transactions on Instrumentation and Measurement,* Vol. 32, 1983, pp. 350-355.

[7] Quinn B.G., Estimating Frequency by Interpolation Using Fourier Coefficients, *IEEE Transactions on Signal Processing,* Vol. 42, 1994, pp. 1264-1268.

[8] Jain V.K., Collins W.L., Davis D.C., High-Accuracy Analog Measurements via Interpolated FFT, *IEEE Transactions on Instrumentation and Measurement*, Vol. 28, 1979, pp. 113-122.

[9] Ding K., Zheng C., Yang Z., Frequency Estimation Accuracy Analysis and Improvement of Energy Barycenter Correction Method for Discrete Spectrum, *Journal of Mechanical Engineering*, Vol. 46, No. 5, 2010, pp. 43-48.

[10] Voglewede P., Parabola approximation for peak determination, *Global DSP Magazine,* Vol. 3, No. 5, 2004, pp. 13-17.

[11] Jacobsen E., Kootsookos P., Fast, accurate frequency estimators, *IEEE Signal Processing Magazine,* Vol. 24, No. 3, 2007, pp. 123-125.

[12] Gillich G.R., Mituletu I.C., *Signal Post-processing for Accurate Evaluation of the Natural Frequencies*. In: Yan R., Chen X., Mukhopadhyay S. (eds), Structural Health Monitoring. Smart Sensors, Measurement and Instrumentation, Vol. 26, Springer Cham, 2017, pp. 13-37.

[13] Ntakpe J.L., Gillich G.R., Mituletu I.C., Praisach Z.I., Gillich N., An accurate frequency estimation algorithm with application in modal analysis, *Romanian Journal of Acoustics and Vibration*, Vol. 13, No. 2, 2016, pp. 98-103.

[14] Gillich G.R., Mituletu I.C., Praisach Z.I., Negru I., Tufoi M., Method to Enhance the Frequency Readability for Detecting Incipient Structural Damage, *Iranian Journal of Science and Technology, Transactions of Mechanical Engineering*, Vol. 41, No. 3, 2017, pp 233–242.

[15] Djukanović S., Popović T., Mitrović A., *Precise sinusoid frequency estimation based on parabolic interpolation*, In Proceedings of the 24th Telecommunications Forum TELFOR, 2016, pp. 1-4.